

Oligomers with complex couplings as \mathcal{PT} -symmetric systems

O. B. Kirikchi

Department of Computing, Goldsmiths, University of London,

New Cross, London SE14 6AD, United Kingdom and

Department of Mathematical Sciences, University of Essex,

Wivenhoe Park, Colchester, Essex CO4 3SQ, United Kingdom

N. Karjanto*

Department of Mathematics, University College, Sungkyunkwan University,

Natural Science Campus, 2066 Seobu-ro, Jangan-gu, Suwon 16419, Gyeonggi-do, Republic of Korea

We consider a chain of dimers with a complex coupling between the arms as parity-time (\mathcal{PT}) symmetric systems. We study fundamental bright discrete solitons of the systems, their existence, and spectral stability. We employ a perturbation theory for small coupling between the arms and small gain-loss parameter to perform the analysis, which is then confirmed by numerical calculations. We consider the fundamental onsite and intersite bright solitons. Each solution possesses symmetric, antisymmetric, and asymmetric configurations between the arms. The stability of the solutions is then determined by solving the corresponding eigenvalue problem. We obtain that all the solitons can be stable for small coupling, on the contrary to the reported continuum limit where the antisymmetric solutions are always unstable. The instability is either due to the internal modes crossing the origin or the appearance of a quartet of complex eigenvalues. In general, the gain-loss term can be considered parasitic as it reduces the stability region of the onsite solitons. Additionally, we analyze the dynamic behavior of the onsite and intersite solitons when unstable, where no traveling solitons nor soliton blow-ups are observed.

I. INTRODUCTION

Dissipative media featuring the parity-time (\mathcal{PT})-symmetry has drawn a great deal of attention ever since the system was proposed by Carl Bender and his collaborators [1–4]. A system of equations is \mathcal{PT} -symmetric if it is invariant with respect to the combined parity (\mathcal{P}) and time-reversal (\mathcal{T}) transformations. The symmetry is fascinating as it forms a particular class of non-Hermitian Hamiltonians in quantum mechanics that may possess a real spectrum up to a critical value of the complex potential parameter, above which the system is in the “broken \mathcal{PT} -symmetry” phase [4–7].

It is assumed that quantities in quantum physics that we observe are the eigenvalues of operators symbolizing the dynamics of the quantities. Therefore, the eigenvalues, which represent the energy spectra should be real and have lower bound so that the system has a stable lowest-energy state. To satisfy such demands, it was speculated that the operators must be Hermitian. Non-Hermitian Hamiltonians have been commonly related to complex eigenvalues and therefore decay of the quantities. However, it turned out that the Hermiticity is not necessarily required by a Hamiltonian system to satisfy the Postulates of Quantum Mechanics [5]. A necessary condition for a Hamiltonian to be \mathcal{PT} -symmetric is that its potential $V(x)$ should satisfy the condition $V(x) = V^*(-x)$ [8].

The most basic configuration of a \mathcal{PT} -symmetric system is a dimer, i.e., an oligomer system of two coupled

oscillators. One of them has damping loses and the other one gains energy from external sources. Indeed, the idea of \mathcal{PT} -symmetry was realized experimentally for the first time on dimers consisting of two coupled optical waveguides [9, 10]. Optical analogs using two coupled waveguides with gain and loss were investigated in [11–13], where such couplers have been already considered previously in the 1990s [14–16].

\mathcal{PT} -symmetric analogs in coupled oscillators have also been proposed theoretically and experimentally [17–20]. A system of coupled oscillators with gain and loss have already been studied [21]. \mathcal{PT} -symmetric system with periodically changing-in-time gain and loss modeled by two coupled Schrödinger equations (dimer) is studied in [22, 23], where a comparison between analytical study and numerical approach were presented to investigate an approximate threshold for \mathcal{PT} -broken symmetry phase corresponding to the disappearance of bounded solutions. A continuum limit of a chain of coupled \mathcal{PT} -symmetric dimers has been covered in [24], where the amplitude system remains conservative and the small-amplitude breathers are stable for a finite time scale. Fascinating class of optical and other systems in which the communication or coupling makes the systems \mathcal{PT} -symmetric was considered in [25], where it discussed the comparison between the dynamical behaviors with that of the usual \mathcal{PT} -symmetric systems with intrinsic loss-gain terms.

In particular, we are interested in the nonlinear dynamics of \mathcal{PT} -symmetric chain of dimers that can be modeled by the discrete nonlinear Schrödinger (DNLS) type of equations due to its abundance applications in nonlinear optics and Bose-Einstein condensates (BEC) [26–28]. Transport on dimers with \mathcal{PT} -symmetric potentials are

* natanael@skku.edu

modeled by the coupled DNLS equations with gain and loss, which was relevant among others to experiments in optical couplers and proposals on BEC in \mathcal{PT} -symmetric double-well potentials [29]. This proposed model is integrable and its integrability is further utilized to build up the phase portrait of the system. The existence and stability of localized mode solutions to nonlinear dynamical lattices of the DNLS type of equations with two-component settings have been considered and a general framework has been provided in [30].

\mathcal{PT} -symmetric systems have also been considered by several authors in various contexts. We present some recent and relevant examples. A system modeling a \mathcal{PT} -symmetric coupler composed by a chain of dimers with a cubic-quintic nonlinearity exhibits a snaking behavior in the bifurcation diagrams for the existence of standing localized solutions [31]. A dual-core nonlinear waveguide with the \mathcal{PT} -symmetry has been expanded by including a periodic sinusoidal variation of the loss-gain coefficients and synchronous variation of the inter-core coupling constant [32]. The system lead to multiple-collision interactions among stable solitons. A study of the nonlinear nonreciprocal dimer in an anti-Hermitian lattice with cubic nonlinearity has been explored recently [33].

In this paper, we consider the coupled discrete linear and nonlinear Schrödinger equations on oligomers with complex couplings as systems of \mathcal{PT} -symmetric potentials. The model arises as nonlinear optical waveguide couplers on BEC in \mathcal{PT} -double well symmetric potentials. The phase portrait of the system and the behavior of the solutions are discussed through analytical and numerical approaches.

The manuscript is outlined as follows. In Section II, we present the equations of motion as the corresponding governing equation. We use perturbation theory for small coupling to analyze the existence of fundamental localized solutions. Such analysis is based on the concept of the so-called anticontinuum limit approach. The stability of the solitons is then considered analytically in Section III by solving a corresponding eigenvalue problem. In addition to small coupling, the expansion is also performed under the assumption of the small coefficient of the gain-loss term due to the non-simple expression of the eigenvectors of the linearized operator. The findings obtained from the analytical calculations are then compared with the numerical counterparts in Section IV. We produce stability regions for the fundamental onsite solitons numerically and present the typical dynamics of solitons in the unstable parameter ranges by direct numerical integrations of the governing equation. We present the conclusion in Section V.

II. MATHEMATICAL MODEL

The governing equations describing \mathcal{PT} -symmetric chains of dimers are of the following form:

$$\begin{aligned}\dot{u}_n &= i|u_n|^2 u_n + i\epsilon\Delta_2 u_n + \gamma v_n + iv_n, \\ \dot{v}_n &= i|v_n|^2 v_n + i\epsilon\Delta_2 v_n - \gamma u_n + iu_n,\end{aligned}\quad (1)$$

where the dots represent the derivative with respect to the evolution variable, which is the physical time t for BEC and the propagation direction z in the case of nonlinear optics. Both $u_n = u_n(t)$ and $v_n = v_n(t)$ are complex-valued wave function at site $n \in \mathbb{Z}$, $0 < \epsilon \ll 1$ is the constant coefficient of the horizontal linear coupling (coupling constant between two adjacent sites), $\Delta_2 u_n = (u_{n+1} - 2u_n + u_{n-1})$ and $\Delta_2 v_n = (v_{n+1} - 2v_n + v_{n-1})$ are the discrete Laplacian terms in one spatial dimension, the gain and loss acting from the complex coupling are represented by the coefficient γ , which without loss of generality can be taken to be $\gamma > 0$. We consider localized solutions satisfying the localization conditions $u_n, v_n \rightarrow 0$ as $n \rightarrow \pm\infty$.

In the uncoupled limit, i.e. when $\epsilon = 0$, the chain (1) becomes the equations for the dimer with complex couplings. This type of \mathcal{PT} -symmetric system with the complex coupling has been studied recently in [25]. A similar setup was studied in [34] in the presence of gain-loss terms, Stokes variable dynamics of the dimer with gain-loss terms were developed as a subcase of a general dimer model. The dimer itself may be considered for the first time in [35, 36], where the integrability was shown.

The focusing system has static solutions that can be obtained from substituting

$$u_n = A_n e^{i\omega t}, \quad v_n = B_n e^{i\omega t}, \quad (2)$$

into (1) to yield the static equations

$$\begin{aligned}\omega A_n &= |A_n|^2 A_n + \epsilon(A_{n+1} - 2A_n + A_{n-1}) - i\gamma B_n + B_n, \\ \omega B_n &= |B_n|^2 B_n + \epsilon(B_{n+1} - 2B_n + B_{n-1}) + i\gamma A_n + A_n,\end{aligned}\quad (3)$$

where A_n, B_n are complex-valued quantities and the propagation constant $\omega \in \mathbb{R}$.

The static equations (3) for $\epsilon = 0$ has been analyzed in details in [25, 35, 36]. When ϵ is nonzero, but sufficiently small, the existence of solutions emanating from the uncoupled limit can be shown using the Implicit Function Theorem (see, e.g., The existence analysis of [29], which can be adopted here rather straightforwardly). However, below we will not state the theorem and instead derive the asymptotic series of the solutions.

Using perturbation expansion, solutions of the coupler (3) for small coupling constant ϵ can be expressed analytically as

$$\begin{aligned}A_n &= A_n^{(0)} + \epsilon A_n^{(1)} + \epsilon^2 A_n^{(2)} + \dots, \\ B_n &= B_n^{(0)} + \epsilon B_n^{(1)} + \epsilon^2 B_n^{(2)} + \dots\end{aligned}\quad (4)$$

By substituting the above expansions into equations (3) and collecting the terms in successive powers of ϵ , one obtains the following equations at $\mathcal{O}(1)$ and $\mathcal{O}(\epsilon)$, respectively

$$\begin{aligned} A_n^{(0)}(1+i\gamma) &= B_n^{(0)}(\omega - B_n^{(0)}B_n^{*(0)}), \\ B_n^{(0)}(1-i\gamma) &= A_n^{(0)}(\omega - A_n^{(0)}A_n^{*(0)}). \end{aligned} \quad (5)$$

and

$$\begin{aligned} A_n^{(1)}(1+i\gamma) &= B_n^{(1)}(\omega - 2B_n^{(0)}B_n^{*(0)}) \\ &\quad - B_n^{(0)2}B_n^{*(1)} - \Delta_2 B_n^{(0)}, \\ B_n^{(1)}(1-i\gamma) &= A_n^{(1)}(\omega - 2A_n^{(0)}A_n^{*(0)}) \\ &\quad - A_n^{(0)2}A_n^{*(1)} - \Delta_2 A_n^{(0)}. \end{aligned} \quad (6)$$

It is well-known two natural fundamental solutions are representing bright discrete solitons that may exist for any ϵ , from the anticontinuum to the continuum limit, i.e. an intersite (two-excited-site) and onsite (one-excited-site) bright discrete mode. Here, we will limit our study to these two fundamental modes.

A. Dimers

In the uncoupled limit $\epsilon = 0$, the time-independent solution of (3), i.e. (5), can be written as $A_n^{(0)} = \tilde{a}_0 e^{i\phi_a}$ and $B_n^{(0)} = \tilde{b}_0 e^{i\phi_b}$, where both amplitudes are positive real valued, i.e. $\tilde{a}_0 > 0$ and $\tilde{b}_0 > 0$. Solving the resulting polynomial equations for \tilde{a}_0 and \tilde{b}_0 will yield [25]

$$\tilde{a}_0 = \tilde{b}_0 = 0, \quad (7)$$

$$\tilde{a}_0 = \tilde{b}_0 = \sqrt{\omega - \sqrt{1 + \gamma^2}}, \quad (8)$$

$$\tilde{a}_0 = -\tilde{b}_0 = \sqrt{\omega + \sqrt{1 + \gamma^2}}, \quad (9)$$

$$\tilde{a}_0 = \frac{1}{\sqrt{2}} \sqrt{\omega + \sqrt{\omega^2 - 4(1 + \gamma^2)}},$$

$$\tilde{b}_0 = \frac{1}{2} \frac{\sqrt{\omega + \sqrt{\omega^2 - 4(1 + \gamma^2)}} [\omega - \sqrt{\omega^2 - 4(1 + \gamma^2)}]}{\sqrt{2(1 + \gamma^2)}}, \quad (10)$$

and the phase $\phi_b - \phi_a = \arctan \gamma$. The parameter ϕ_a can be taken as 0, due to the gauge phase invariance of the governing equation (1) and henceforth $\phi_b = \arctan(\gamma)$. Solutions (8), (9), and (10) are referred to as the symmetric, antisymmetric, and asymmetric solutions, respectively. The asymmetric solution (10) emanates from a pitchfork bifurcation from the symmetric solution (8) at $\omega = 2\sqrt{1 + \gamma^2}$.

Another variant of interesting dimers where the coupling between the oscillators provide a gain to the system was considered in [37–39]. Such a system may model the propagation of electromagnetic waves in coupled waveguides embedded in an active medium. The dimer considered herein when $\epsilon \rightarrow 0$ is different as in our case the

coupling between the cores not only provide gain but also loss.

B. Intersite solitons

The mode structure of the intersite solitons in the anticontinuum limit is given by

$$\begin{aligned} A_n^{(0)} &= \begin{cases} \tilde{a}_0 & n = 0, 1, \\ 0 & \text{otherwise,} \end{cases} \\ B_n^{(0)} &= \begin{cases} \tilde{b}_0 e^{i\phi_b} & n = 0, 1, \\ 0 & \text{otherwise.} \end{cases} \end{aligned} \quad (11)$$

For the first-order correction due to the weak coupling, writing $A_n^{(1)} = \tilde{a}_1$, $B_n^{(1)} = \tilde{b}_1 e^{i\phi_b}$, and substituting these into equations (6) will yield

$$\begin{aligned} \tilde{a}_1 &= \frac{\tilde{b}_1(\omega - 3\tilde{b}_0^2) + \tilde{b}_0}{\sqrt{1 + \gamma^2}}, \\ \tilde{b}_1 &= \frac{\tilde{a}_1(\omega - 3\tilde{a}_0^2) + \tilde{a}_0}{\sqrt{1 + \gamma^2}}, \end{aligned} \quad (12)$$

Equations (11) and (12) are the asymptotic expansions of the intersite solitons. One can continue the same calculation to obtain higher-order corrections, which we will omit here as considering the first two terms is already sufficient for our analysis.

C. Onsite solitons

For the onsite soliton, i.e., a one-excited-site discrete mode, one can perform the same computations to obtain the mode structure of the form

$$\begin{aligned} A_n^{(0)} &= \begin{cases} \tilde{a}_0 & n = 0, \\ 0 & \text{otherwise,} \end{cases} \\ B_n^{(0)} &= \begin{cases} \tilde{b}_0 e^{i\phi_b} & n = 0, \\ 0 & \text{otherwise,} \end{cases} \end{aligned} \quad (13)$$

and the first-order correction from (6)

$$\begin{aligned} \tilde{a}_1 &= \frac{\tilde{b}_1(\omega - 3\tilde{b}_0^2) + 2\tilde{b}_0}{\sqrt{1 + \gamma^2}}, \\ \tilde{b}_1 &= \frac{\tilde{a}_1(\omega - 3\tilde{a}_0^2) + 2\tilde{a}_0}{\sqrt{1 + \gamma^2}}. \end{aligned} \quad (14)$$

The asymptotic expansions of the onsite solitons are thus given by equations (13) and (14). Likewise, higher-order corrections can be obtained using a similar calculation.

III. STABILITY ANALYSIS

In the following, we consider six configurations, which are combinations of the intersite and onsite discrete solitons with the three solutions of the dimers (8)–(10). We

will denote them by subscripts i and o for intersite and onsite solitons, and s , at , and as for the symmetric, antisymmetric, and asymmetric solutions, respectively.

After we find discrete solitons, their linear stability is then determined by solving the corresponding linear eigenvalue problem.

To do so, we introduce the linearisation ansatz $u_n = (A_n + \tilde{\epsilon}(K_n + iL_n)e^{\lambda t})e^{i\omega t}$, $v_n = (B_n + \tilde{\epsilon}(P_n + iQ_n)e^{\lambda t})e^{i\omega t}$, $|\tilde{\epsilon}| \ll 1$, and substitute this into Eq. (1) to obtain the linearised equations at $\mathcal{O}(\tilde{\epsilon})$

$$\begin{aligned} \lambda K_n &= -(A_n^2 - \omega)L_n - \epsilon(L_{n+1} - 2L_n + L_{n-1}) + \gamma P_n - Q_n, \\ \lambda L_n &= (3A_n^2 - \omega)K_n + \epsilon(K_{n+1} - 2K_n + K_{n-1}) + \gamma Q_n + P_n, \\ \lambda P_n &= -[\text{Re}^2(B_n) + 3\text{Im}^2(B_n) - \omega]Q_n - \epsilon(Q_{n+1} - 2Q_n + Q_{n-1}) - 2\text{Re}(B_n)\text{Im}(B_n)P_n - \gamma K_n - L_n, \\ \lambda Q_n &= (3\text{Re}^2(B_n) + \text{Im}^2(B_n) - \omega)P_n + \epsilon(P_{n+1} - 2P_n + P_{n-1}) + 2\text{Re}(B_n)\text{Im}(B_n)Q_n - \gamma L_n + K_n, \end{aligned} \quad (15)$$

which have to be solved for the eigenvalue λ and the corresponding eigenvector $\{K_n\}, \{L_n\}, \{P_n\}, \{Q_n\}\}^T$. The solution u_n is said to be (linearly) stable when $\text{Re}(\lambda) \leq 0$ for all the spectra λ and unstable otherwise. However, as the spectra will come in pairs, a solution is therefore stable when $\text{Re}(\lambda) = 0$ for all $\lambda \in \mathbb{R}$.

A. Continuous spectrum

The spectrum of (15) will consist of continuous and discrete spectra (eigenvalues). To investigate the former, we consider the limit $n \rightarrow \pm\infty$, introduce the plane-wave ansatz $K_n = \hat{k}e^{ikn}$, $L_n = \hat{l}e^{ikn}$, $P_n = \hat{p}e^{ikn}$, $Q_n = \hat{q}e^{ikn}$, $k \in \mathbb{R}$, and substitute the ansatz into (15) to obtain

$$\lambda \begin{bmatrix} \hat{k} \\ \hat{l} \\ \hat{p} \\ \hat{q} \end{bmatrix} = \begin{bmatrix} 0 & \xi & \gamma & -1 \\ -\xi & 0 & 1 & \gamma \\ -\gamma & -1 & 0 & \xi \\ 1 & -\gamma & -\xi & 0 \end{bmatrix} \begin{bmatrix} \hat{k} \\ \hat{l} \\ \hat{p} \\ \hat{q} \end{bmatrix} \quad (16)$$

where $\xi = \omega - 2\epsilon(\cos k - 1)$. The matrix equation (16) can be solved analytically to yield the dispersion relation

$$\lambda^2 = -(1 + \gamma^2) - \xi^2 \pm 2|\xi|\sqrt{1 - \gamma^2}. \quad (17)$$

The continuous spectrum is therefore given by $\lambda \in \pm[\lambda_{1-}, \lambda_{2-}]$ and $\lambda \in \pm[\lambda_{1+}, \lambda_{2+}]$ with the spectrum boundaries

$$\lambda_{1\pm} = \pm i\sqrt{1 + \gamma^2 + \omega^2 \mp 2|\omega|\sqrt{1 + \gamma^2}}, \quad (18)$$

$$\lambda_{2\pm} = \pm i\sqrt{1 + \gamma^2 + (\omega + 4\epsilon)^2 \mp 2|\omega + 4\epsilon|\sqrt{1 + \gamma^2}}, \quad (19)$$

obtained from (17) by setting $k = 0$ and $k = \pi$ in the equation.

B. Discrete spectrum

Following the weak-coupling analysis as in Section II, we will as well use similar asymptotic expansions to solve the eigenvalue problem (15) analytically, i.e., we write

$$X = X^{(0)} + \sqrt{\epsilon}X^{(1)} + \epsilon X^{(2)} + \dots, \quad (20)$$

with $X = \lambda, K_n, L_n, P_n, Q_n$. We then substitute the expansions into the eigenvalue problem (15).

At order $\mathcal{O}(1)$, one will obtain the stability equation for the dimer, which has been discussed for a general value of γ in [25]. The expression of the eigenvalues is simple, but the expression of the corresponding eigenvectors is not, which makes the result rather impractical to use. Therefore, here we limit ourselves to the case of small $|\gamma|$ and expand (20) further as

$$X^{(j)} = X^{(j,0)} + \gamma X^{(j,1)} + \gamma^2 X^{(j,2)} + \dots,$$

$j = 0, 1, 2, \dots$. Hence, we have two small parameters, i.e. ϵ and γ , that are independent of each other. The steps of finding the eigenvalues $\lambda^{(j,k)}$, $j, k = 0, 1, 2, \dots$ have been outlined in details in [23]. Here, we will present the results.

1. Intersite soliton

We have three types of intersite solitons (i.e., symmetric, antisymmetric, and asymmetric ones). All of them have in general one pair of eigenvalues that bifurcate from the origin for small ϵ and two pairs of nonzero eigenvalues. They are asymptotically given by

$$\lambda_{i,s} = \sqrt{\epsilon} (2\sqrt{\omega - 1} - \gamma^2 / (2\sqrt{\omega - 1}) + \dots) + \mathcal{O}(\epsilon), \quad (21)$$

$$\lambda_{i,at} = \sqrt{\epsilon} (2\sqrt{\omega + 1} + \gamma^2 / (2\sqrt{\omega + 1}) + \dots) + \mathcal{O}(\epsilon), \quad (22)$$

$$\lambda_{i,as} = \sqrt{\epsilon} (2\sqrt{\omega} + \dots) + \mathcal{O}(\epsilon), \quad (23)$$

for the eigenvalues bifurcating from the origin and

$$\lambda_{i,s} = \begin{cases} \left(2\sqrt{\omega-2} + \gamma^2 \frac{\omega-4}{2\sqrt{\omega-2}} + \dots \right) + \epsilon \left(\sqrt{\omega-2} - \gamma^2 \frac{\omega}{4\sqrt{\omega-2}} + \dots \right) + \mathcal{O}(\epsilon^{3/2}), \\ \left(2\sqrt{\omega-2} + \gamma^2 \frac{\omega-4}{2\sqrt{\omega-2}} + \dots \right) + \epsilon \left(\frac{1}{\sqrt{\omega-2}} + \gamma^2 \frac{\omega}{4(\omega-2)^{3/2}} + \dots \right) + \mathcal{O}(\epsilon^{3/2}), \end{cases} \quad (24)$$

$$\lambda_{i,at} = \begin{cases} \left(2i\sqrt{\omega+2} + \gamma^2 \frac{i(\omega+4)}{2\sqrt{\omega+2}} + \dots \right) - \epsilon \left(i\sqrt{\omega+2} + \gamma^2 \frac{3i(\omega^2+5\omega+4)}{8(\omega+2)^{3/2}} + \dots \right) \\ + \mathcal{O}(\epsilon^{3/2}), \\ \left(2i\sqrt{\omega+2} + \gamma^2 \frac{i(\omega+4)}{2\sqrt{\omega+2}} + \dots \right) + \epsilon \left(\frac{i}{\sqrt{\omega+2}} + \gamma^2 \frac{i(5\omega^2+21\omega+12)}{8(\omega+2)^{3/2}} + \dots \right) \\ + \mathcal{O}(\epsilon^{3/2}), \end{cases} \quad (25)$$

$$\lambda_{i,as} = \begin{cases} \left(\sqrt{4-\omega^2} - \gamma^2 \frac{2i}{\sqrt{\omega^2-4}} + \dots \right) + \epsilon \left(\frac{3i\omega}{\sqrt{\omega^2-4}} + \gamma^2 \frac{6i\omega}{(\omega^2-4)^{3/2}} + \dots \right) + \mathcal{O}(\epsilon^{3/2}), \\ \left(\sqrt{4-\omega^2} - \gamma^2 \frac{2i}{\sqrt{\omega^2-4}} + \dots \right) + \epsilon \left(\frac{i\omega}{\sqrt{\omega^2-4}} + \gamma^2 \frac{2i\omega}{(\omega^2-4)^{3/2}} + \dots \right) + \mathcal{O}(\epsilon^{3/2}), \end{cases} \quad (26)$$

for the nonzero eigenvalues.

2. Onsite soliton

Similarly, we also have three types of onsite solitons with each one generally has only one nonzero eigenvalue

for small ϵ given asymptotically by

$$\lambda_{o,s} = \left(2\sqrt{\omega-2} + \gamma^2 \frac{(\omega-4)}{2\sqrt{\omega-2}} + \dots \right) + \epsilon \left(\frac{2}{\sqrt{\omega-2}} + \gamma^2 \frac{\omega}{2(\omega-2)^{3/2}} + \dots \right) + \mathcal{O}(\epsilon^{3/2}), \quad (27)$$

$$\lambda_{o,at} = \left(2i\sqrt{\omega+2} + \gamma^2 \frac{i(\omega+4)}{2\sqrt{\omega+2}} + \dots \right) + \epsilon \left(\frac{2i}{\sqrt{\omega+2}} + \gamma^2 \frac{i\omega}{2(\omega+2)^{3/2}} + \dots \right) + \mathcal{O}(\epsilon^{3/2}), \quad (28)$$

$$\lambda_{o,as} = \left(i\sqrt{\omega^2-4} - \gamma^2 \frac{2i}{\sqrt{\omega^2-4}} + \dots \right) + \epsilon \left(\frac{2i\omega}{\sqrt{\omega^2-4}} + \gamma^2 \frac{4i\omega}{(\omega^2-4)^{3/2}} + \dots \right) + \mathcal{O}(\epsilon^{3/2}). \quad (29)$$

IV. NUMERICAL RESULTS

We have solved the steady-state equation (3) numerically using a Newton-Raphson method and analyzed the stability of the numerical solution by solving the eigenvalue problem (15). Below we will compare the analytical calculations obtained above with the numerical results.

First, we consider the discrete intersite symmetric soliton. We show in the top panels of Figure 1 the spectrum of the soliton as a function of the coupling constant ϵ for $\omega = 2$ and $\gamma = 0.5$. The dynamics of the non-zero eigenvalues as a function of the coupling constant are shown in the right panels of the figure, where one can see that firstly there is only one eigenvalue and as the coupling increases, one of the nonzero eigenvalues that was initially on the imaginary axis becomes real, too.

In the bottom panels of the same figure, we plot the eigenvalues for ω large enough. Here, in the uncoupled limit, all the three pairs of eigenvalues are on the real axis. As the coupling increases, two pairs go back toward the origin, while one pair remains on the real axis

(not shown here). In the continuum limit $\epsilon \rightarrow \infty$, we, therefore, obtain an unstable soliton (i.e., an unstable symmetric soliton). In both figures, we also plot the approximate eigenvalues in solid (blue) curves, where good agreement is obtained for small ϵ .

Next, we consider antisymmetric intersite solitons. Figure 2 shows a typical distribution of the spectra in the complex plane of the discrete solitons for one particular value of ω . There is an eigenvalue bifurcating from the origin. For the selected value of ω we choose here, we have the condition that the nonzero eigenvalues λ satisfy $\lambda^2 < \lambda_{2-}^2$ in the anticontinuum limit $\epsilon \rightarrow 0$. The collision between the eigenvalues and the continuous spectrum as the coupling increases creates complex eigenvalues. Additionally, in the continuum limit the value of ω as well as other values of the parameter that we computed for this type of discrete solitons yield unstable solutions.

The final case for intersite solitons is the asymmetric one. Figure 3 displays a common spectrum distribution in the complex plane for a particular choice of parameters ω and γ . Although the complex eigenvalues are

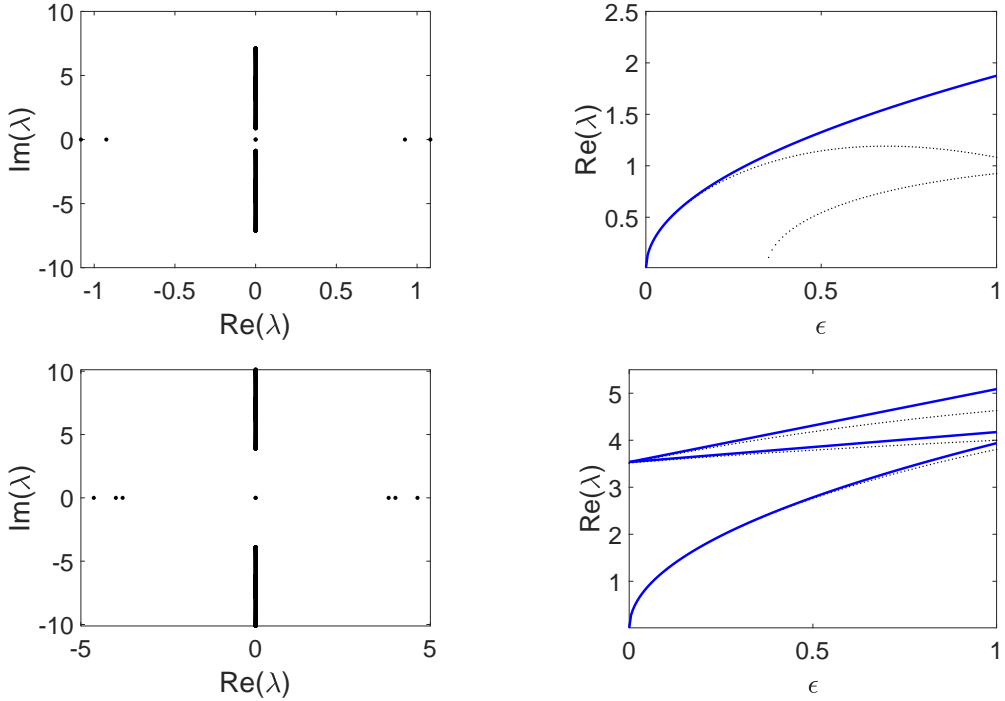


FIG. 1. The spectra of intersite symmetric soliton with $\omega = 2$, $\gamma = 0.5$ (top panels) and $\omega = 5$, $\gamma = 0.9$ (bottom panels). The left panels are the spectra in the real plane for $\epsilon = 1$. Right panels present the eigenvalues as a function of the coupling constant. The solid blue curves are the asymptotic approximations presented in Subsubsection III B 1 while the dots are obtained from a numerical calculation.

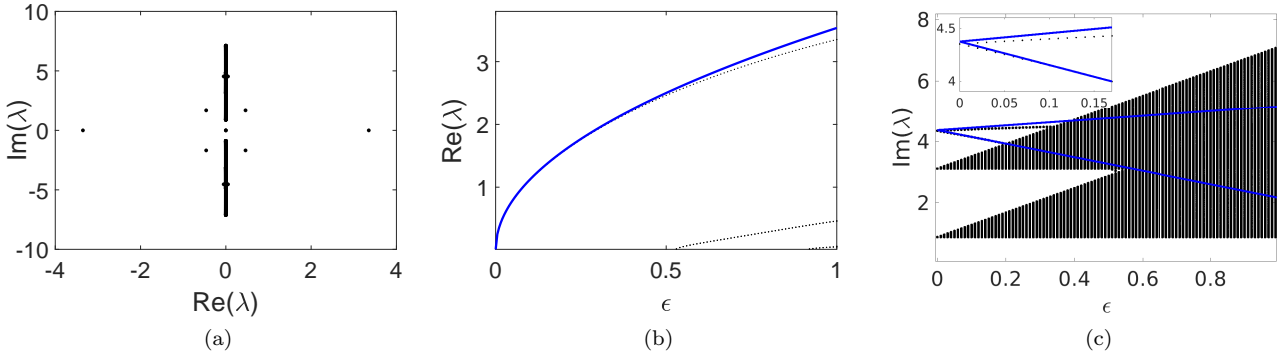


FIG. 2. The spectra of antisymmetric intersite soliton with $\omega = 2$ and $\gamma = 0.5$. Panel (a) displays the spectra in the complex plane for $\epsilon = 1$. Panels (b) and (c) present the eigenvalues λ as a function of the coupling constant ϵ . The solid blue and dotted curves are attained from the asymptotic approximation and numerical calculation, respectively.

not visible, the asymmetric intersite solitons yield unstable solutions for the set of calculated parameters in the continuum limit. In the anticontinuum limit, the position of the discrete spectrum for the previous case of the antisymmetric intersite is above all the continuous spectrum, *viz.* Figure 2. The main interesting part is that the unstable eigenvalues bifurcate into the complex plane, *i.e.*, the emergence of eigenvalues with non-zero imaginary part. For the asymmetric intersite case, the position of the discrete spectrum is in between the con-

tinuous one and the imaginary part remains zero.

We also study onsite solitons shown in Figures 4–6. Unlike intersite discrete solitons that are always unstable, onsite discrete solitons may be stable. In Figure 4(a), we show the spectrum as a function of the coupling. The choice of ω , in this case, corresponds to stable discrete solitons. However, there are regions of instability for different parameter values of ω that may depend on γ and ϵ . We present the (in)stability region of the discrete solitons in the (ϵ, ω) -plane for three values of the gain-loss parameter γ in Figure 4(b). Onsite symmetric discrete solitons

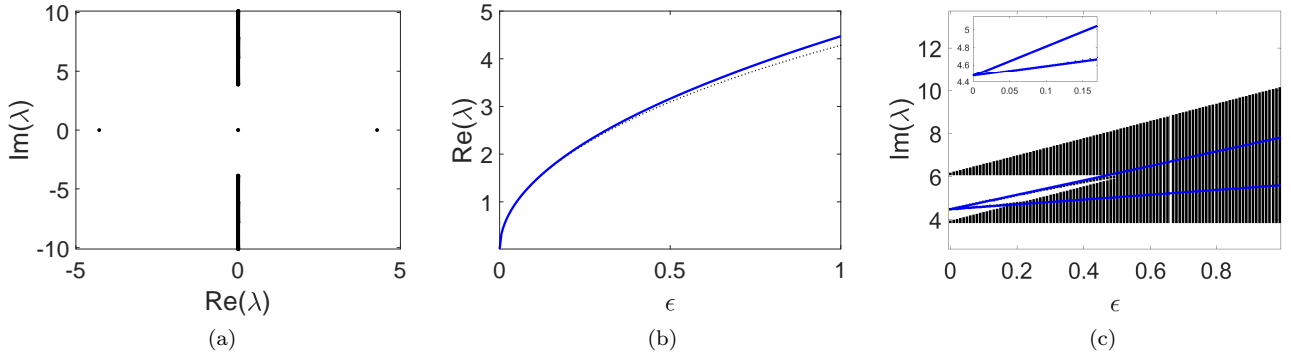


FIG. 3. The spectra of asymmetric intersite soliton with $\omega = 5$ and $\gamma = 0.5$. Panel (a) displays the spectra in the real plane for $\epsilon = 1$. Panels (b) and (c) present the eigenvalues λ as a function of the coupling constant ϵ . The solid blue and dotted curves are attained from the asymptotic approximation and numerical calculation, respectively.

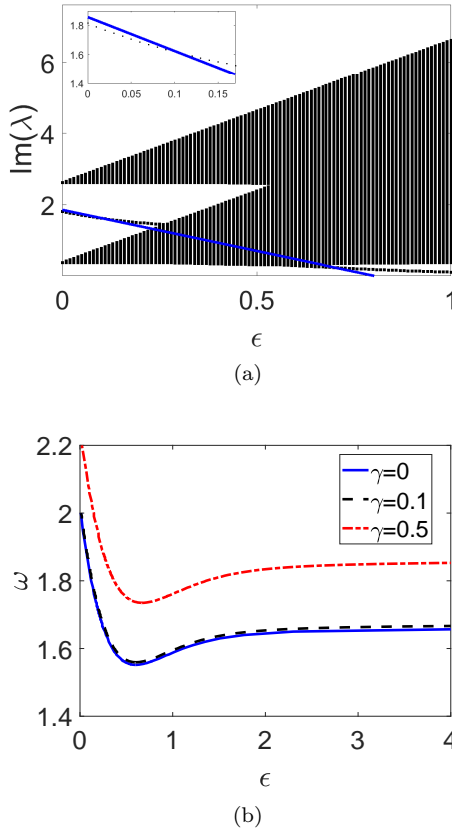


FIG. 4. (a) Eigenvalues as a function of the coupling and its approximation of symmetric onsite soliton with $\omega = 1.5$, $\gamma = 0.5$. (b) The stability region of the onsite soliton in the (ϵ, ω) -plane for several values of γ . The solutions are unstable above the curves.

are unstable above the curves. In general, we obtain that the gain-loss term in the coupling can be beneficial as it increases the stability region of the discrete solitons.

Figure 5 shows that the antisymmetric solitons are gen-

erally unstable due to a quartet of complex eigenvalues, as shown in the left panels of the figure. As the instability is due to the collision of an eigenvalue with the continuous spectrum, stability regions may present prior to the collision. Panel (c) shows the region, where antisymmetric solitons are unstable between the curves. These solitons are unstable in the continuum limit. Figure 6 shows asymmetric solitons that are stable in the region of their existence. Note that this soliton bifurcates from symmetric ones.

Finally, we present in Figures 7–10 the time dynamics of the unstable solutions shown in Figures 1–5. What we obtain is that typically there is only one dynamics, i.e. in the form of discrete soliton destructions. One may obtain oscillating solitons or asymmetric solutions between the arms.

V. CONCLUSION

We have presented a systematic method to determine the stability of discrete solitons in a \mathcal{PT} -symmetric coupler by computing the eigenvalues of the corresponding linear eigenvalue problem using asymptotic expansions. We have compared the analytical results that we obtained with numerical computations, where good agreement is obtained. From the numerics, we have also established the mechanism of instability as well as the stability region of the discrete solitons. The application of the method in higher dimensional \mathcal{PT} -symmetric couplers is a natural extension of the problem that is addressed for future work.

ACKNOWLEDGEMENT

We are grateful to Professor Hadi Susanto, Department of Mathematical Sciences, University of Essex, UK and Department of Mathematics, Khalifa University, Abu Dhabi, The United Arab Emirates for his assistance and valuable comments in improving this paper significantly.

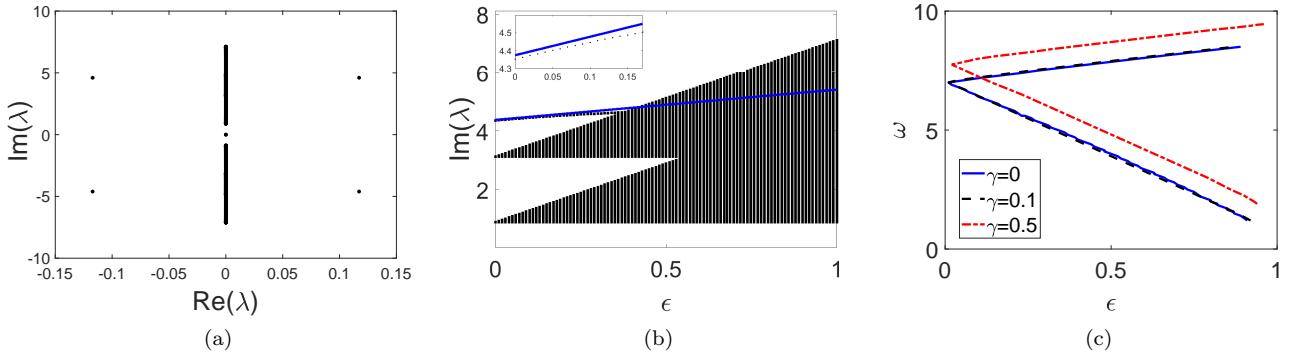


FIG. 5. Panels (a) and (b) display eigenvalues of antisymmetric onsite soliton for $\omega = 2$, $\gamma = 0.5$, and $\epsilon = 1$. (c) The stability diagram of the discrete solitons for several values of γ . Antisymmetric solitons are unstable between the curves.

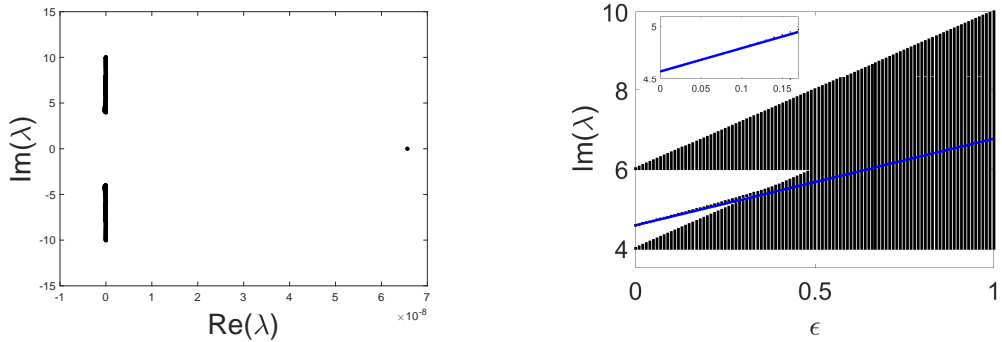


FIG. 6. Eigenvalues of asymmetric onsite soliton for $\omega = 5$, $\gamma = 0.1$, and $\epsilon = 1$. The right-panel shows stability in their existence region.

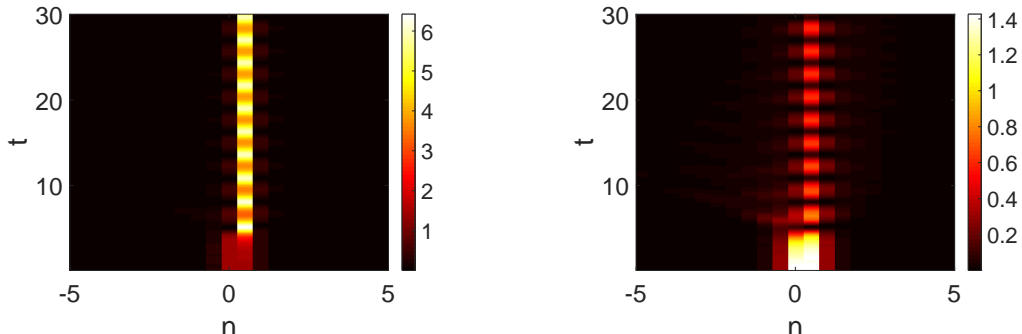


FIG. 7. The typical dynamics of unstable symmetric discrete intersite solitons with $\omega = 2$, $\gamma = 0.5$, $\epsilon = 1$ (see Figure 1). Depicted in the left and right panels are $|u_n|^2$ and $|v_n|^2$, respectively.

[1] C. M. Bender and S. Boettcher, Phys. Rev. Lett. **80**, 5243 (1998).
[2] C. M. Bender, S. Boettcher, and P. N. Meisinger, J. Math. Phys. **40**(5), 2201 (1999).
[3] C. M. Bender, D. C. Brody, and H. F. Jones, Phys. Rev. Lett. **89**, 270401 (2002).
[4] C. M. Bender, Rep. Prog. Phys. **70**, 947 (2007).
[5] N. Moiseyev, *Non-Hermitian Quantum Mechanics* (Cambridge University Press, UK, 2011).
[6] T. Kottos, Nat. Phys. **6**(3), 166 (2010).
[7] D. D. Scott, and Y. N. Joglekar, Phys. Rev. A **83**(5), 050102(R) (2011).
[8] J. Pickton, and H. Susanto, Phys. Rev. A **88**, 063840 (2013).

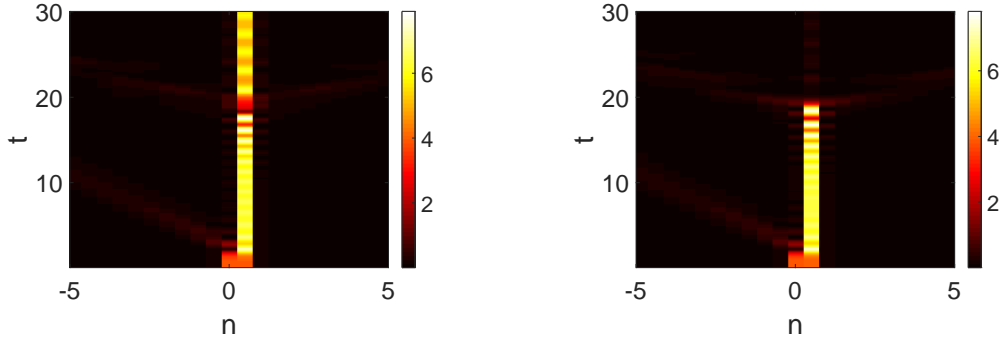


FIG. 8. The same as Figure 7, but for an unstable antisymmetric discrete intersite soliton with the same parameter values.

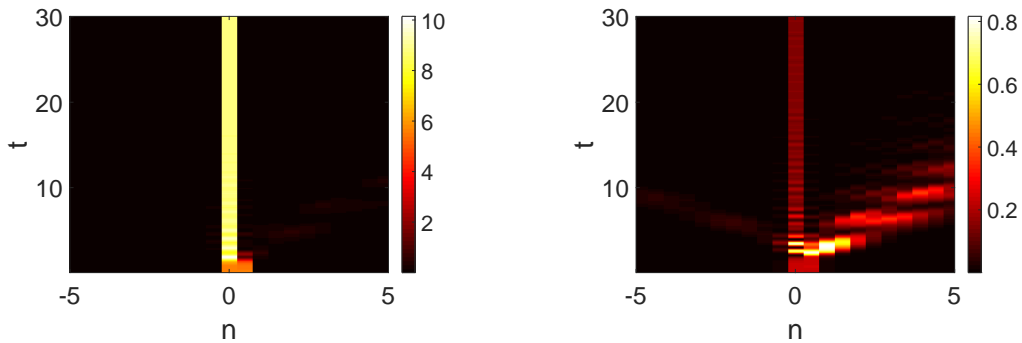


FIG. 9. The typical dynamics of asymmetric discrete intersite solitons with $\omega = 5$, $\gamma = 0.5$, $\epsilon = 1$.

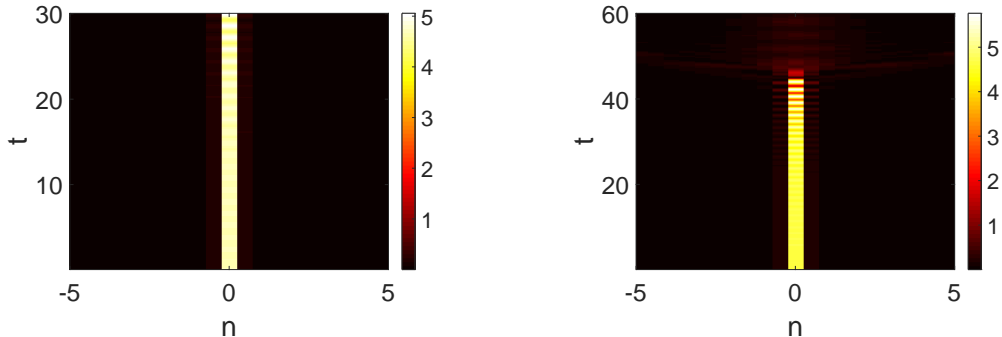


FIG. 10. The typical dynamics of antisymmetric onsite solitons with $\omega = 2$, $\gamma = 0.5$, $\epsilon = 1$.

- [9] A. Guo, G. J. Salamo, D. Duchesne, R. Morandotti, M. Volatier-Ravat, V. Aimez, G. A. Siviloglou, and D. N. Christodoulides, *Phys. Rev. Lett.* **103**, 093902 (2009).
- [10] C. E. Rüter, K. G. Makris, R. El-Ganainy, D. N. Christodoulides, M. Segev, and D. Kip, *Nat. Phys.* **6**, 192 (2010).
- [11] A. Ruschhaupt, F. Delgado, and J. G. Muga, *J. Phys. A* **38**, L171 (2005).
- [12] R. El-Ganainy, K. G. Makris, D. N. Christodoulides, and Z. H. Musslimani, *Opt. Lett.* **32**, 2632 (2007).
- [13] S. Klaiman, U. Günther, and N. Moiseyev, *Phys. Rev. Lett.* **101**, 080402 (2008).
- [14] Y. Chen, A. W. Snyder, and D. N. Payne, *Quantum Electronics* **28**, 239 (1992).
- [15] M. F. Jørgensen, P. L. Christiansen, and I. Abou-Hayt, *Physica D* **68**, 180 (1993).
- [16] M. J. Jørgensen and P. L. Christiansen, *Chaos, Solitons & Fractals* **4**, 217 (1994).
- [17] J. Schindler, A. Li, M. C. Zheng, F. M. Ellis, and T. Kottos, *Phys. Rev. A* **84**, 040101(R) (2011).
- [18] H. Ramezani, J. Schindler, F. M. Ellis, U. Günther, and T. Kottos, *Phys. Rev. A* **85**, 062122 (2012).
- [19] Z. Lin, J. Schindler, F. M. Ellis, and T. Kottos, *Phys. Rev. A* **85**, 050101(R) (2012).
- [20] J. Schindler, Z. Lin, J. M. Lee, H. Ramezani, F. M. Ellis, and T. Kottos, *J. Phys. A: Math. Theor.* **45**, 444029 (2012).

- [21] P. J. Holmes, and J. E. Marsden, *Comm. Math. Phys.* **82**, 523 (1982).
- [22] F. Battelli, J. Diblík, M. Fečkan, J. Pickton, M. Pospíšil, and H. Susanto, *Nonlin. Dyn.* **81** 1 (2015).
- [23] O. B. Kirikchi, A. A. Bachtiar, and H. Susanto, *Adv. Math. Phys.* **2016**, 9514230 (2016).
- [24] I. V. Barashenkov, S. V. Suchkov, A. A. Sukhorukov, S. V. Dmitriev, and Y. S. Kivshar, *Phys. Rev. A* **86**(5), 053809 (2012).
- [25] S. Karthiga, V. K. Chandrasekar, M. Senthilvelan, and M. Lakshmanan, *Phys. Rev. A* **94**, 023829 (2016).
- [26] P. G. Kevrekidis, K. Ø. Rasmussen, and A. R. Bishop, *Int. J. Mod. Phys. B* **15**(21), 2833 (2001).
- [27] Y. S. Kivshar and G. Agrawal, *Optical Solitons: From Fibers to Photonic Crystals*, Fourth edition (Academic Press, Cambridge, Massachusetts, 2003).
- [28] P. G. Kevrekidis, *The Discrete Nonlinear Schrödinger Equation: Mathematical Analysis, Numerical Computations, and Physical Perspectives* (Vol. 232, Springer Science & Business Media, Berlin Heidelberg, Germany, 2009).
- [29] A. Chernyavsky and D. E. Pelinovsky, *Symmetry* **8**, 59 (2016).
- [30] K. Li, P. G. Kevrekidis, H. Susanto, and V. Rothos, *Math. Comp. Simul.* **127**, 151 (2012).
- [31] H. Susanto, R. Kusdiantara, N. Li, O. B. Kirikchi, D. Adzkiya, E. R. M. Putri, and T. Asfihani, *Phys. Rev. E* **97**(6), 062204 (2018).
- [32] Z. Fan and B. A. Malomed, *Comm. Nonlin. Sci. Numer. Simul.* **79**, 104906 (2019).
- [33] S. Tombuloglu and C. Yuce, *Comm. Nonlin. Sci. Numer. Simul.* **83**, 105106 (2020).
- [34] H. Xu, P. G. Kevrekidis, and A. Saxena, *J. Phys. A: Math. Theor.* **48**, 055101 (2015).
- [35] M. F. Jørgensen, P. L. Christiansen, and I. Abou-Hayt, *Physica D* **68**, 180 (1993).
- [36] M. F. Jørgensen and P. L. Christiansen, *Chaos, Solitons & Fractals* **4**, 217 (1994).
- [37] N. V. Alexeeva, I. V. Barashenkov, K. Rayanov, and S. Flach, *Phys. Rev. A* **89**, 013848 (2014).
- [38] B. Dana, A. Bahabad, and B. A. Malomed, *Phys. Rev. A* **91**, 043808 (2015).
- [39] O. B. Kirikchi, B. A. Malomed, N. Karjanto, R. Kusdiantara, and H. Susanto, *Phys. Rev. A* **98**(6), 063841 (2018).